Influence of Polymer Architecture and Polymer−Surface Interaction on the Elution Chromatography of Macromolecules through a Microporous Media

C. M. Guttman,* E. A. Di Marzio, and J. F. Douglas

Polymers Division, National Institute of Standards and Technology, Gaithersburg, Maryland 20899

Received February 8, 1996; Revised Manuscript Received May 6, 1996[⊗]

ABSTRACT: The elution chromatography of flexible polymer molecules flowing through a microporous particle media is described by a combination of the Casassa model of flow segregation and the Di Marzio−Rubin lattice method for calculating the partition function of confined polymers. This combination of models allows for the treatment of polymer-surface interactions so that polymer chromatography in the exclusion and adsorption regimes can be described within a unified framework. The compensation point where repulsive polymer-surface excluded volume forces and short-range polymer-surface attractive forces counterbalance each other offers opportunities for separating complex molecules. For example, calculations for a diblock copolymer where one of the components is at the compensation point ("adsorption Θ point") indicate that only the remaining block influences the elution of the block copolymer as a whole. This theoretical result accords with experiments on block copolymers. This singular observation provides support for the Casassa viewpoint of molecular partitioning dominated polymer elution. The chromatography of triblock copolymers, stars, and combs is also examined to determine the selectivity of elution chromatography for separating these molecular architectures. The theoretical development in the present paper should lead to improved methods for the characterization of polymers with different molecular architectures. These developments also suggest new tools for studying polymer adsorption from dilute solution.

1. Introduction

There are many applications of molecular segregation phenomena associated with the flow of polymer molecules through porous media. In general, these segregation processes reflect an interplay between hydrodynamic and thermodynamic effects which often allow remarkably effective separations. The primary factors which control molecular separation are the geometry of the porous media and the interaction between the polymer and the solid substrate. In practice many aspects of molecular separation remain an art since the theory of flow-induced separation has been rather idealized.

Theoretical models of molecular separation under flow have primarily focused on the influence of repulsive interactions between the polymer and the solid matrix of the flow medium. In a capillary flow, for example, the exclusion of the polymer or other solvated species from the wall causes such particles to lie closer to the center of the capillary where the fluid velocity is higher. (This same physics occurs for a fluid flowing through a hole or a screen, but the velocity increase near the center of the apertures is not as great.) Di Marzio and Guttman[1−3] have developed this simple concept of volume exclusion between capillary wall and dissolved polymers into a theory of flow-induced polymer separation which is appropriate for porous media with channel-like structures where the pores have a relatively uniform cross-section. This model predicts that high molecular weight polymers elute through the matrix first because of the greater excluded volume interference between the pore surface and the polymer.

Casassa introduced another model of flow-induced polymer separation based on the polymer−substrate excluded volume concept.[4−6] Real porous media are often characterized by cul-de-sac type pores which lie off the main channels in which flow is concentrated. This situation is predominant in situations in which the porous media itself is comprised of microporous particles in which the polymers in solution can partition. If the cul-de-sac pore size is not large relative to the mean dimensions of the flexible polymer chain, then there is an entropic cost for the polymers to enter the pores associated with a repulsive interaction between the polymer and the pore surface. This leads to a partitioning of the polymers between the pores and the flowing solvent exterior to the microporous surface. Casassa has made convincing arguments that this type of molecular segregation occurs under flow conditions leading to flow-induced molecular segregation.[4,5] As in the case of flow separation in capillaries, the high molecular weight polymers elute first because excluded volume interactions between the polymer and the pore increase with the molecular weight of the polymer.

The exclusion chromatography models of Di Marzio and Guttman and of Casassa are complementary models which are appropriate for different types of porous media. Real porous media often involve a combination of channel structures and microporous solid particles so that both hydrodynamic and thermodynamic processes can be expected to operate in molecular segregation in the case of the flow of polymer solutions through general porous media.

An attractive interaction between the polymer in solution and the solid portion of the porous medium can substantially affect molecular separation. The attractive interaction counterbalances the excluded volume until a compensation point is obtained, "the adsorption Θ point"(see below), where the excluded volume effect between the polymer and the flow matrix vanishes. Selective molecular separation with flow is lost at this compensation point (see Figure 1). For an even greater attractive polymer matrix interaction, the polymer

[⊗] Abstract published in *Advance ACS Abstracts,* July 1, 1996.

S0024-9297(96)00202-1

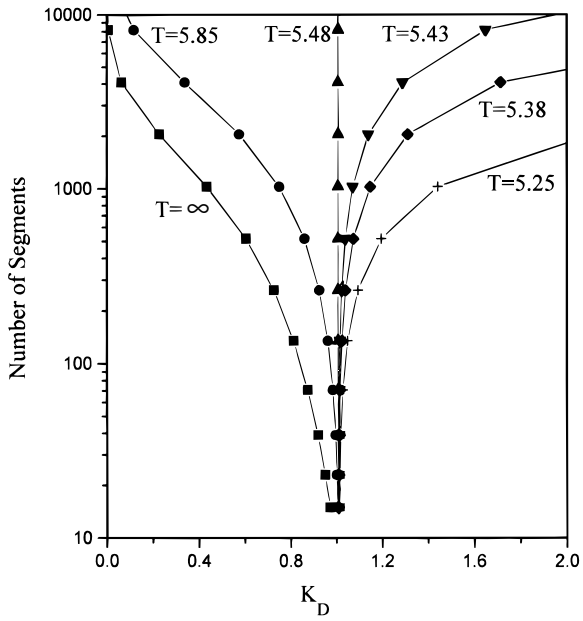

Figure 1. Partition coefficient, K_D, for a homopolymer in a slit-like pore of a width of 50 units computed by the Di Marzio−Rubin lattice method. The compensation point occurs at the temperature $T = 5.48$ for a chain on a cubic lattice. The partition coefficient K_D is independent of molecular weight at the compensation point. (This temperature is also called the adsorption Θ point or "adsorption transition point" for a chain of infinite length.) The shape and general features of the curves on this figure correspond well to the experimental elution volume data of Pasch et al.[14]

becomes adsorbed onto the surface of the matrix so that the higher molecular weight polymers exhibit an inhibited flow through the porous media (see Figure 1). This qualitative phenomenon is rather independent of the geometry of the porous medium except to the degree to which the polymer−flow matrix interaction is influenced by the geometry of the porous medium (see below).

In the present paper we focus on the role of attractive polymer-surface interactions in the Casassa model since this model is appropriate to describing molecular separation in porous media composed of rigid microporous particles. This model is also convenient because it can be combined with the Di Marzio−Rubin lattice model of polymers confined between interacting surfaces[7] so that the influence of simultaneous variation in molecular architecture and polymer surface interaction can be explored with this model.

Since the polymer−surface compensation point of different polymers in a diluted blend or of different blocks of monomers within a block copolymer are different and the polymer surface interaction can be tuned through the mixing of solvents and/or the variation of temperature, it is possible to achieve molecular separation of blends and block copolymers and to infer important features of molecular structure from elution measurements. The possibilities for molecular selectivity in block copolymers of various architectures are explored in this paper theoretically.

Although this paper is focused on the calculation of the mean value of the peak position in the elution chromatography of a polymer, a more complete analysis would consider the entire peak shape. Early on, Hermans derived formulas for both the mean value of the elution volume and the Gaussian distribution about the mean,[8] thereby justifying the Casassa viewpoint of partitioning in size exclusion chromatography (SEC) of polymers. Guttman and Di Marzio extended this approach to the case of flow-through pores as well as dead-end pores and determined the third moment[3] (skewness). Weiss has used concepts of trapping to model the partitioning of an eluent between the flowing and mobile phases.[9] This method allows the eluent adsorbed into or onto the stationary phase or phases to elute out of the phase/phases according to a phenomenological trapping function (memory kernel). In this treatment, situations in which the average residence time, $\langle t \rangle$, is infinite, corresponding to some non-zero fraction of the material remaining in the column, are easily treated. The Weiss treatment should prove useful when the system is on the adsorption side of the compensation point.

An even simpler approach to understanding the basics of SEC is a development using the convolution theorem and the central limit theorem to obtain the average elution volume and peak spreading of a polymer molecule in an SEC column of N plates in terms of the probability distribution describing the elution of the individual plates themselves. This technical matter is considered in Appendix A.

2. Elution Chromatography through a Microporous Particle Media

A. The Casassa Model of Flow Segregation. In the Casassa chromatography model of flow segregation of polymers through equilibrium partitioning, the average elution volume reflects the quasi-equilibrium partitioning of the polymer between a flowing "mobile phase" and "stationary phase". The stationary phase corresponds to the solution within the bead pores in which the polymers are localized, while the mobile phase corresponds to the region outside the pores where large-scale transport occurs. The average elution volume V_e in this simple model is given by the additive relation

$$V_e = V_m + K_D V_p \tag{2.1}$$

where V_m is the mobile phase volume, V_p is the total pore volume, and K_D is the equilibrium partition coefficient (see below). For SEC, K_D is less than 1, while for normal adsorption chromatography, K_D is greater than 1.

Entelis and others[10,11] have studied the chromatography of homopolymers experimentally, particularly end-functionalized "telechelic" homopolymers, from the size exclusion range through the adsorption range by varying solvent composition in a mixed solvent system. A compensation point is found where the partition coefficients of a homologous homopolymer series equal unity. At the compensation point, polymers of all molecular weights have the same elution volume. Thus, the column has no selecting effect on the polymers. The elution volume of the polymers at their compensation point is also the elution volume of the solvent.

Pasch has used this method to investigate the chromatography of polymer blends.[12] By choosing a solvent system in which one component of the blend has $K_D = 1$ while the other is in the exclusion range, he obtained the molecular weight distribution of one blend component without interference from the other component. Pasch et al.[13,14] and Zimina et al.[15] have also studied an AB diblock copolymer consisting of a B portion that is at its compensation point ($K_D = 1$ for the block alone) and an A portion that is in the exclusion regime. The

elution volume obtained from the chromatogram of such a diblock was found to display only the molecular weight dependence of the A block so that the B portion was effectively "invisible" to the column. Similarly, if the composition of the mixed solvent is at the compensation point for the A portion and the B portion is in the exclusion range, then the influence of the A portion is suppressed; only the B portion is visible to the column. This method has also been applied to the characterization of triblock copolymers.[16] These observations provide a demonstration of how the compensation point can be used to mask the influence of portions of the polymer chain in elution chromatography.

All these observations are consistent with the Casassa quasi-equilibrium model of molecular partitioning in a microporous separating media. Accordingly, in this paper we develop a systematic approach to calculating the partition coefficient of confined polymers of various architectures and compositions to further explore the selectivity of this type of chromatography to molecular architecture.

B. Theoretical Models of Chain Confinement and Polymer−Surface Interaction. The theory of flow-induced molecular separation in the Casassa model is based on the calculation of the partition coefficient K_D in eq 2.1. The partition coefficient K_D under equilibrium conditions is equal to the ratio of the partition function in a pore, Q_{pore}, to the partition function of the "free polymer" in bulk solution, Q_{free}. Under the quasi-equilibrium conditions within a chromatographic column, K_D is approximated by the ratio Q_{pore} to the chain partition function in the mobile phase, Q_{mobile}. The mobile phase is that region outside the pore space of the particles forming the chromatographic substrate. Thus, we have the basic relation

$$K_D = Q_{pore}/Q_{mobile} \approx Q_{pore}/Q_{free} \qquad (2.2)$$

Casassa's original modeling of K_D considered only the exclusion interaction regime corresponding to repulsive polymer−surface interaction. His model accounted for both linear and star architectures based on a continuum Gaussian chain model.[4] Entelis et al.[10] has recently reviewed the extension of continuous chain modeling to the case of polymer chains having attractive polymer surface interactions. This work emphasized telechelic polymers having end groups whose interaction with the surface is different from the rest of the polymer. More recent work by Skvortsov et al.[17,18] and Gorshkov et al.[19] has generalized the continuum polymer chain models to copolymers as well.

Although the continuum models provide important qualitative insights into molecular partitioning in elution chromatography when there are attractive polymer−surface interactions, there are aspects of the molecular phenomena which are better described by the lattice model calculations. Specifically, the factors which govern the critical temperature for adsorption cannot be calculated on the basis of continuum theory and the continuum theory gives unphysical results for certain properties when the polymer−surface interaction is strongly attractive.[20] More importantly for the present paper, the continuum model allows for only a limited discussion of chain architecture variation on K_D. The Di Marzio−Rubin lattice theory[7] of confined surface interacting polymers, on the other hand, lends itself readily to the study of essentially arbitrary molecular architecture variations, confinement, and polymer−surface interactions. These are the details which are essential in using elution chromatography as a quantitative tool for separating complex molecules.

C. Assumptions and Limitations of the Chromatography Model. The modeling in the present paper is based on a number of idealizations in addition to the adoption of the Casassa model of molecular separation by flow. In this section we discuss some of the other factors which should ultimately be included in a more molecularly faithful model of elution chromatography. We also take this opportunity to define some nomenclature before developing our detailed model of molecular partitioning in the next section.

First, we must recognize the complex structure of the pore space in real chromatographic materials and that any particular model of the pore shape necessitates idealization. Fortunately, there are general mathematical limit theorems which govern the free energy change of confined polymers.[21] Regardless of the mode of confinement (cylinder, slit, sphere, ...), the free-energy change of confinement ΔF in the long chain limit has the asymptotic form

$$K_D = Q_{pore}/Q_{free} = \exp(-\Delta F/kT) \sim \exp(-\lambda_1 n), \qquad n \to \infty \qquad (2.3)$$

for flexible polymer chains where n is the polymerization index (proportional to molecular weight) and λ_1 is an eigenvalue. In the exclusion regime and the continuum chain limit, λ_1 is inversely related to the first-passage time of a random walk to encounter the boundary for a walk which starts within a region having essentially arbitrary shape.[22] For ordinary random walks the mean-square displacement increases proportional to the time-like variable n so that λ_1 scales as

$$\lambda_1 \sim 1/L^2 \qquad (2.4)$$

where L is a characteristic dimension defining the average size of the region in which the chain is confined.[22] Explicit calculations by Casassa for idealized geometries (slit, cylinder, sphere)[4,6,23] provide examples of the general scaling relationship in eq 2.4. Casassa also calculates the constant of proportionality for these special geometries.

Since the particular geometrical form of confinement influences only the nonuniversal constant of proportionality in eq 2.4, we have some freedom in choosing a model of confinement based on mathematical expediency. The particular geometrical model of chain confinement within a pore should not affect the qualitative estimates of the partition coefficients, which is fortunate given the complex form of the real pore space. The slit geometry which we consider in the present paper captures the salient features of the reduction of chain degrees of freedom due to the confinement and should serve as a minimal model to describe the confinement effect. Equations 2.3 and 2.4 have also been used to develop a theory of rubber elasticity of confined networks based on a similar philosophy.[24]

The neglect of polymer−polymer excluded volume interaction is a shortcoming of our modeling and most other modeling of polymer elution chromatography. However, Monte Carlo calculations show that many of the essential features of molecular partitioning are uninfluenced by segment−segment excluded volume interaction. There is a shift in the critical temperature

which accords with expectations[25] based on the entropy change per link of self-avoiding chains versus random walk chains and the exact calculation of critical temperature for adsorption of simple random walks by Rubin.[26] This is not a complication in our modeling since the critical temperature is determined experimentally. Numerical calculations show that eq 2.3 is also obtained for self-avoiding walk (SAW) chains, but the scaling in eq 2.4 becomes modified as[27]

$$\lambda_1 \sim 1/L^{1/\nu} \tag{2.5}$$

where ν describes the scaling of average SAW chain size R with chain length n,

$$R \sim n^{\nu}, \qquad \nu \approx 10/17 \tag{2.6}$$

The asymptotic scaling relation eqs 2.3 and 2.5 are also important in connection with finite-size corrections in second-order phase transitions (see Appendix B).

The general limit theorem eq 2.3 also obtains when attractive polymer−surface interactions exist which are sufficient to adsorb the polymer. In this case the confinement scale L in eq 2.4 is replaced by a correlation length describing the thickness of the adsorbed layer.[28] The sign of the eigenvalue λ_1 becomes reversed in the adsorbed chain regime so that the partition coefficient becomes much greater than unity and high molecular weight elution through the column is inhibited. Direct measurements of log K_D for polystyrene with a silica particle gel substrate for a series of mixed solvents ranging from the exclusion to the adsorption regime[29] exhibit a linear dependence on molecular weight, as indicated by eq 2.3, which provides an important consistency check on the Casassa model of elution chromatography and the insensitivity of the phenomenology to solvent quality.

The condition $K_D = 1$ is often identified as a "critical point" of polymer adsorption and chromatography in the interaction range where $K_D \approx 1$ is often termed "critical chromatography". This identification is correct in the limit of infinite chains, but for finite chains (i.e., real chains) adsorption occurs at *lower* temperatures which depend on chain length.[30] The condition $K_D = 1$ actually defines a compensation point where attractive and repulsive interactions counterbalance each other, and this condition is exactly analogous to the Θ point of polymer solutions.[30] This connection is apparent from considering the difference $A_1 \equiv K_D - 1$,

$$A_1 = Q_{\text{pore}}/Q_{\text{free}} - 1 \tag{2.7}$$

which is an analog of the definition of the second virial coefficient,[30] A_2, for interacting polymer where Q_{pore} is replaced by the partition function of the two interacting chains and Q_{free} is the square of the single chain self-interacting polymer partition function. Equation 2.7 is effectively a "first virial coefficient"[31] describing the interaction between the polymer and the substrate. The relation between the adsorption Θ point and the conventional Θ point for polymer excluded volume is discussed in previous work.[25,32]

There are two other factors left out of our model of molecular partitioning which can be important in some circumstances—chain rigidity and the roughness of the gel matrix. The adsorption Θ point $K_D = 1$ and the Θ point for polymer interactions ($A_2 = 0$) are influenced by chain stiffness.[33] The dependence of the compensation point for polymer adsorption on stiffness is evident. Little chain conformational entropy is involved in adsorbing polymer chains from solution. However, confinement of a real chain to a pore can alter the chain rigidity[34] and thus influence the effective polymer surface interaction if the confinement effect is large. Kholodenko et al.[35] have recently treated the confinement of semiflexible chains between interacting parallel plates. Numerical calculations by Davidson et al.[36] suggest that chain flexibility can have an appreciable influence on molecular partitioning. In practice we expect semiflexibility effects to be important for studies involving a large range of molecular weights since semiflexibility varies with chain length in short polymer chains and for pores which have a scale on the order of the statistical segment length. Semiflexibility effects can be readily incorporated into the Di Marzio−Rubin[7] lattice model but shall not be explored further in this paper.

The roughness of the matrix can also influence the adsorption Θ point if the roughness pattern occurs over a wide range of scales[37] (i.e., fractal type structures). This should not complicate the case of model porous media having pores with a relatively narrow range of sizes, however. Explicit calculations show that the scale of confinement[38] and smooth variations of boundary shape have little influence on the adsorption transition temperature.[39]

As a final reservation about comparison with experiment we note that the experimental procedure of varying the polymer−solvent interaction through the use of solvent mixtures is not well understood theoretically. The phenomena observed in the chromatography experiments does suggest that the primary influence of using mixed solvents is to alter the surface interaction. As discussed above, part of this effect must derive from an alteration of the polymer−polymer excluded volume interaction, which in turn can affect the adsorption Θ point. Any preferential absorption of the polymer by one of the components would affect the absorption Θ point. Furthermore, the occupation of the surface sites at random by the components of the fluid mixture should also modify the potential of mean local polymer−surface interaction. The tendency of particular components to wet or preferentially associate with particular parts of the surface are complications in practice for such mixed solvent polymer solutions.

3. Matrix Method Calculation of K_D for Homopolymers, Block Copolymers, Stars, and Combs.

The Di Marzio−Rubin lattice model allows for the calculation of the ratio of the partition function of a chain in a slit to the same chain in solution. Thus, the Di Marzio−Rubin model yields K_D for a confined polymer. We next apply the matrix method of calculating K_D to describing the elution chromatography of homopolymers, copolymers, and branched molecules such as stars and combs. The sensitivity of molecular segregation near the compensation point is particularly examined to estimate the possibilities for achieving molecular separation through control of the polymer surface interaction.

The partition function, $Q(m,N)$, of a random walk homopolymer of N repeat units starting at level m away from the surface but confined between two parallel plates is given by

$$Q(m,N) = \mathbf{U}_m \mathbf{q}(\theta)^{N-1} \mathbf{P}(0)/M \tag{3.1}$$

The partition coefficient for the same homopolymer

without the end constraint equals

$$K_D(N) = \sum_m Q(m,N) = \mathbf{U}\mathbf{q}(\theta)^{N-1}\mathbf{P}(0)/M \quad (3.2)$$

where M is, as before, the plate separation, $\mathbf{U}_m$ is the row vector with all zeros except a single 1 in the mth position, $\mathbf{U}$ is the row vector with all 1's , $\mathbf{P}(0)$ is the column vector (e^{θ}, 1, ..., 1, e^{θ}), and the matrix $\mathbf{q}(\theta)$ is defined as

$$\mathbf{q}(\theta) = \begin{pmatrix} (1-a)e^{\theta} & {}^1/_2 a e^{\theta} & & & & & \\ {}^1/_2 a & 1-a & {}^1/_2 a & & & & \\ & {}^1/_2 a & 1-a & {}^1/_2 a & & & \\ & & {}^1/_2 a & 1-a & & & \\ & & & & \ddots & & \\ & & & & 1-a & {}^1/_2 a & \\ & & & & {}^1/_2 a & 1-a & {}^1/_2 a \\ & & & & & {}^1/_2 a e^{\theta} & (1-a)e^{\theta} \end{pmatrix} \quad (3.3)$$

where $\theta = \epsilon/kT$, ϵ is the energy of adsorption for a monomer contacting the surface and $a/2$ is the fraction of steps toward or away from the confining surface. Different lattices are treated by proper choice of a. In this paper we will choose a three-dimensional cubic lattice where $a = {}^1/_3$. M is the total number of layers including the plate walls. One can also allow for arbitrary energies $\epsilon(m)$, where m is the layer number, by multiplying each row of the matrix by $\exp[\epsilon(m)/kT]$. One can also model the internal stiffness energies of the chain to whatever level of approximation is required.[7,40]

The extension of the Di Marzio–Rubin lattice method to block copolymers has particular interest for chromatography. For the present study, we assume each different kind of monomer of the block copolymer interacts with the surface with an energy ϵ_A or ϵ_B and that each chain walks on the same cubic lattice ($a_A = a_B$). Again disregarding interactions within the solution, we obtain for a block copolymer of n_A consecutive repeats of A-type monomers and n_B consecutive repeats of B-type monomers the partition coefficient K_D

$$K_D(R,S) = U\mathbf{q}(\theta_A)^{n_A}\mathbf{q}(\theta_B)^{n_B}P(0)/M \quad (3.4)$$

where $\mathbf{q}(\theta_A)$ is the matrix of the A monomers and $\mathbf{q}(\theta_B)$ is the matrix of the B monomers. Extensions to other linear chain architectures are obvious. All that is necessary is to retain in eq 3.4 the same sequence that exists in the polymer chain. Further, since we can make calculations for branched, graft and star homopolymers and ring polymers,[40,41] it is obvious we can also consider copolymers having these more complex architectures.

A. K_D for Homopolymers. We first consider a homopolymer molecule in a solvent with varying solvent strength or temperature. We examine K_D as a function of temperature (when we refer to a variation of "temperature", we additionally imply varying the polymer surface interaction ϵ by using mixed solvents, pressure, etc.). The partition coefficient for a plate separation of 50 lattice units is shown in Figure 1. This numerical calculation is to be compared with the experimental data in Figure 1 of Pasch et al.[13]

The qualitative features of the experimental data of Pasch et al. and those of our model are very similar. We notice the Pasch et al. data at low molecular weight has the entire exclusion regime and the absorption regime squeezed into the region near $K_D = 1$ since there is limited effect of confinement on the free energy. This is where the solvent is expected to elute. For SEC the solvent and polymer elute at the same volume when the number of monomers in the polymer approaches unity. The vertical line is for $K_D = 1$ for all molecular weights. This means that for this polymer–carrier solvent combination the column cannot separate the polymer from the solvent. As shown below, this feature provides a basis for making one component of a diblock copolymer invisible while separating the diblock based on the molecular weight of the other component.

A notable feature of both the experimental curves and the theoretical curves is their large information content. The variation of volume elution with composition of solvent is a new dimension of information that we, along with the previous workers in the field, now seek to exploit. The challenge is to use this information to determine the structure and composition of the polymer molecules.

B. K_D for Diblocks. We next consider a diblock copolymer. One block, A, has n_A segments with only exclusion interactions with the wall and the B block has n_B segments with both attractive and exclusion interactions with the wall. For the block whose monomers have attractive interactions with the wall we look at attractive energies equivalent to $T = 5.48$ ($\epsilon/k \equiv 1$), which is the compensation point for the infinitely long chain on a cubic lattice.

Figure 2 shows K_D for these chains versus the logarithm of the length n_A of the A block which is the block with zero energy of attraction to the wall and the B block which is at the compensation point. As we see, there is no effect on the chromatogram due to variation of the number of B segments, n_B, on the K_D of the diblock copolymer. The K_D of the AB block copolymer is independent of the number of segments with attractive interactions if we are at the transition or compensation point. Within this model, the column should be effectively "invisible" to the block of B's in the copolymer. We are looking at the molecular weight distribution of the A block only. Alternatively, if we use a solvent for which the A component is masked, we could separate the molecules from the B component alone. Thus, the use of mixed solvent carriers allows us to examine the internal structure of the diblock copolymer.

These theoretical results agree with the chromatographic data of Pasch et al.[13] and Zimina et al.[15] In their experiments on diblock copolymers Pasch et al. found that the molecular weight distribution of the A polymer determined by SEC is unaffected by the presence of the B block provided the solvent mixture is adjusted so that the system is at the adsorption compensation point of the B component. Thus, both theory and experiment conclude that the presence of the block B at its compensation point does not affect the elution volume of the excluded chains. This singular observation provides support for the Casassa model of the chromatographic separation which is based entirely on an equilibrium partition concept.

C. Effect of Pore Size on AB Diblock Partitioning. Since the columns used in this chromatography

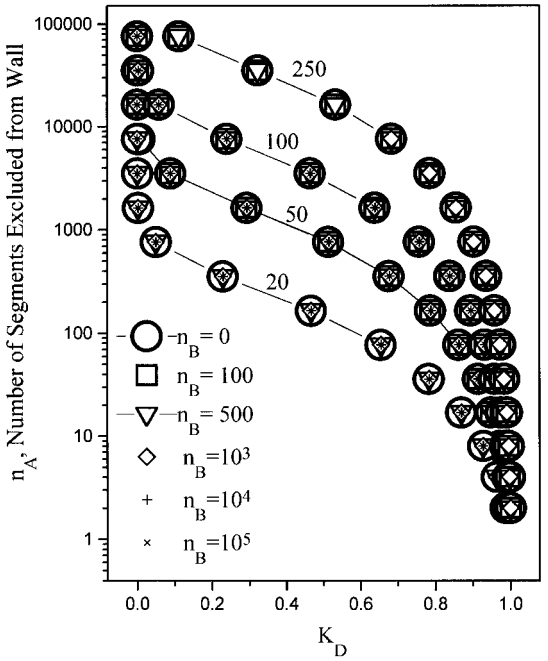

Figure 2. Partition coefficient K_D for an A−B diblock copolymer. n_A A monomers in the DiMarzio−Rubin lattice method are excluded from the wall, while n_B B monomers are at the compensation point, $T = 5.48$. The curves are seen to be independent of the number of monomers in the B portion of the chain. This shows that the molecular weight distribution of the A's in the presence of the B's can be obtained chromatographically by masking the B component. These calculations are made for slit widths ranging from 20 to 250 lattice spacings.

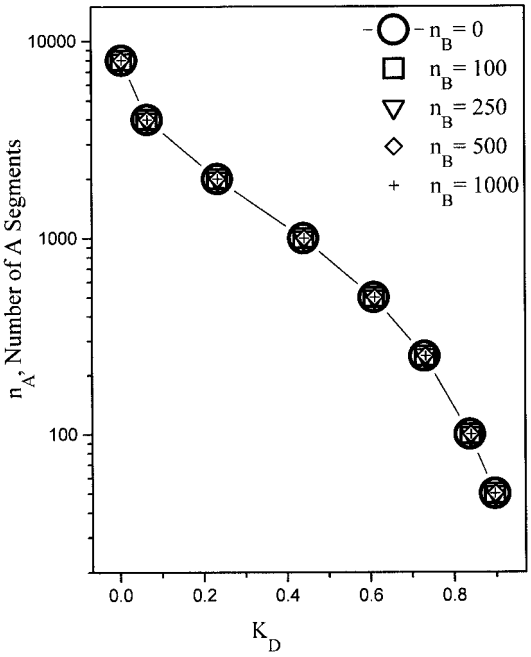

Figure 3. Partition coefficient K_D for a B−A−B triblock copolymer in a slit of 50 lattice spacings. The A monomers are excluded from the wall, and the B monomers are at their transition point $T = 5.48$ of the homopolymer of B segments. n_A is the number of A monomers, and n_B is the number of B monomers in each block. The number of B's in each block varies from zero to 1000 with no apparent change on the value of the K_D for the various values of A. This shows we can obtain the molecular weight distribution of the A's in the presence of the B's for a B−A−B triblock where the B blocks are masked.

do not have a single pore size, we need to consider the effect of pore size on the position of the compensation point and on K_D. Casassa[42] found that the pore size dramatically affects the partition coefficient in the surface exclusion regime. In the fully absorbed case of the polymer the partition function is little affected by pore size since the polymer is adsorbed against the pore wall. In the adsorption regime the effect of pore size has been studied by Di Marzio and Rubin.[7] They showed that slit separation, M, had little effect on the compensation point. This is evidently a consequence of the fact that when the polymers are strongly adsorbed onto the surface, the segments of the chain do not contact the other boundary unless the other surface is very close to the surface onto which the segments are adsorbed.

For an AB block we see in Figure 2 that for slits from widths of 20−250 there is no effect of the making of the polymer invisible; and the calibration curve for the part that is not invisible is independent of the size of the invisible block. The same is expected to be true for the BAB triblock where the B is the masked section.

D. Numerical Treatment of BAB Triblocks. We next consider two cases of triblock copolymers. In one case the block with no attraction to the wall is the center block (BAB). In the other case the blocks with no attraction to the wall are the outside blocks (ABA). Obviously, by proper choice of solvent any triblock copolymer can be transformed into the other. However, from the point of view of the chromatography, this distinction is important because triblocks with an "invisible" center behave differently than triblocks with "invisible" ends.

In Figure 3 we show the data for a BAB triblock that has the A groups with no attraction to the wall and the B blocks with attraction to the wall, but at the compensation point for the B blocks. Again, we see there is no effect of the existence of the B blocks on the SEC of the A block. This form of chromatography allows us to see into the interior of the triblock. This result is similar to the diblock case and is expected. The experimental data of Gorshkov et al.[16] on poly(ethylene oxide-*block*-propylene oxide) shows this behavior.

E. Numerical Treatment of ABA Triblocks. We now consider the ABA triblock where as before the A blocks have no attraction to the walls and the interior B block is the masked block. The two A blocks are chosen to have the same size in this example. In Figure 4 we plot K_D at the compensation point of the B block against the total number of A's for various lengths of B. The first observation is that there is no simple superposition as there was for the BAB triblock. These curves nearly superpose, but not quite. The superposition is closer to the chains with a smaller number of B's than with a larger number of B's. Thus, the approximation

$$K_{D,ABA} = K_{D,2A} \tag{3.5}$$

holds rather well for chains having short B lengths. The partition function, $K_{D,2A}$, is the exact partition coefficient for a chain whose B length equals zero, i.e., the homopolymer of length 2A.

We can also consider the effect of varying the B length from the extreme where the A blocks are unattached from one another. This situation should be a good approximation to the case where the B length is very long compared to the slit width and leads to the approximation

$$K_{D,ABA} = (K_{D,A})^2 \tag{3.6}$$

Data for the ABA triblock plotted with the approxima-

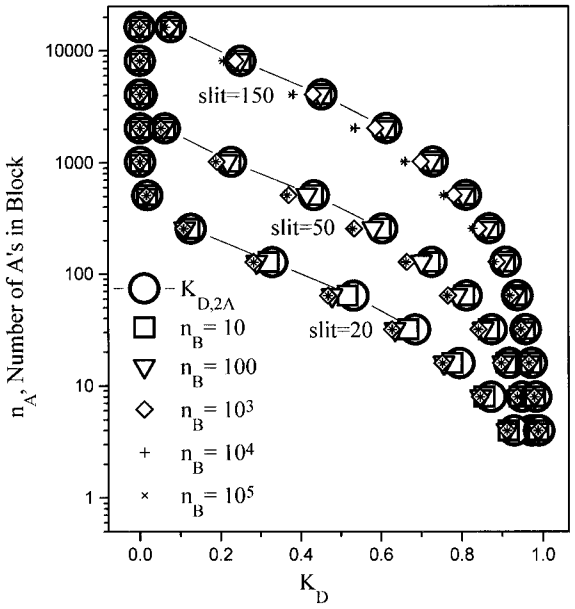

Figure 4. Partition coefficient K_D for an A−B−A triblock copolymer for slit widths of 20, 50, and 150 lattice spacings. The A monomers are excluded from the wall, and the B monomers are at their compensation point, $T = 5.48$. This shows the effect of two A chains tied together by a phantom B chain. The number of B's varies from zero to 100 000. The partition function for the A chain with zero B monomers (a homopolymer of 2A monomers) is shown by open circles in the figure. The homopolymer of 2A monomers best represents the partition function with varying phantom B's for ABA blocks provided n_B is small.

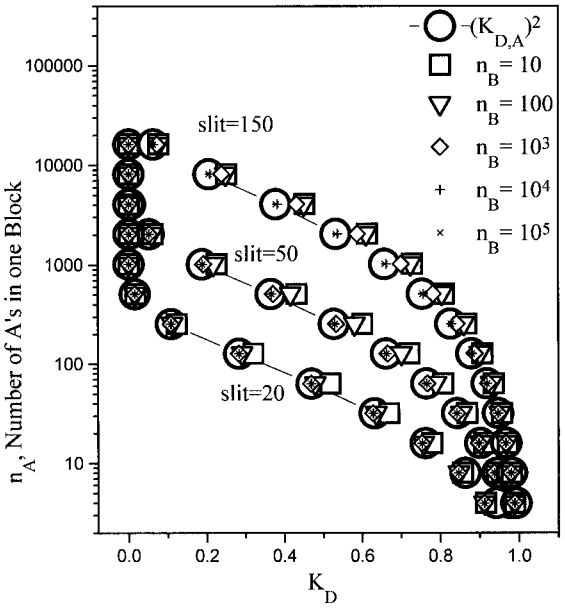

Figure 5. Partition coefficient K_D for an A−B−A triblock copolymer for slit widths of 20, 50, and 150 units. The A monomers are excluded from the wall, and the B monomers are at their transition point, $T = 5.48$. The number of B's varies from 10 to 10 000 monomers. The partition function for the A chain with no B monomer is significantly different from the ones with the B block in the chain. This figure shows the effect of assuming that the two A chains tied by a phantom B chain between are uncorrelated. The K_D of two uncorrelated chains then equals $K_{D,ABA} = K_{D,A}^2$. The partition function of the ABA chain as the product of the partition function of the two blocks of A each of length n_A is shown by an open circle. As seen from the figure, this model is a good representation of the data when n_B is large.

tion in eq 3.6 are plotted in Figure 5. Here the equation is best fit with data with the chains with large B lengths.

From the above discussion, we see that the effect of making B invisible in the ABA triblock is not as easy to interpret as in the diblock case or in the BAB triblock case. In the first place varying the molecular weight of the B component results in slightly different curves, so that the B component is no longer invisible. Using either model, the curves do provide a good rough indication of the triblock copolymer partition coefficient.

F. Effect of Pore Size on Partition Coefficients of ABA Triblocks. What is the effect of wall separation in the triblock case? In earlier sections numerical work for triblocks with separations of 50 lattice units only was discussed. Much larger separation, 150 lattice units, and much smaller ones, 20 lattice units, are shown in Figures 4 and 5. As we increase or decrease the plate separation, ABA copolymer chains with small B blocks are modeled best by models in which we assume that the two A chains are joined, i.e., are correlated. This is seen in Figure 4. This is not true for the uncorrelated model in Figure 5. As we increase the plate separation, the "squared model", eq 3.6, shows significant deviation for all chain sizes. We have put a block of B 10 000 units long in the ABA triblock in this plot, and we see that for a plate separation of 150 the curve is beginning to approach the model line. On the other hand, if we make the separation 20, then we see that all but the smallest length of the B block give a good fit to the model.

The above discussion suggests that the loss of correlation as envisioned by the model above is a result of the combination of the size of the B block and the plate separation and pore size. This is consistent with results we found earlier on the effect of separation in a dilute solution of strong bonds (chain segments which had attractions to the wall) in polymer made up of weak bonds (chain segments which were only excluded from the wall). In this work we found that the effects arising from the strong bonds became independent of their concentration in the pore—losing memory of the actual concentration of the strong bonds.[41] The data on the ABA triblock copolymers are consistent with this view.

G. K_D for Stars. Using $Q(m,N)$ from eq 3.1, we can define $Q_i(m,N_i)$ to be the partition function for the ith chain of the star, which consists of N_i segments and which begins at level m. Then, the partition function for the star is given by

$$Q(\text{star}) = \sum_m \prod_i Q_i(m,N_i) \qquad (3.7)$$

Each arm of the star can be a homopolymer, a copolymer, or a comb polymer. This equation has been discussed previously.[41]

We first consider if the absorption Θ point of the homopolymer star is changed resulting from the architecture of the star. In Figure 6 we show the absorption compensation point for homopolymer stars when the number of arms varies from 2 to 6. The temperature is set at the adsorption compensation point for the infinite homopolymer, $T^* = 5.48$ where the homopolymer is expected to have $K_D = 1$ for any long chain. We see in Figure 6 that there is only a small change in the compensation point due to the number of arms. Overall there are very small changes in the K_D as we increase the number of arms, K_D changing less then 1%.

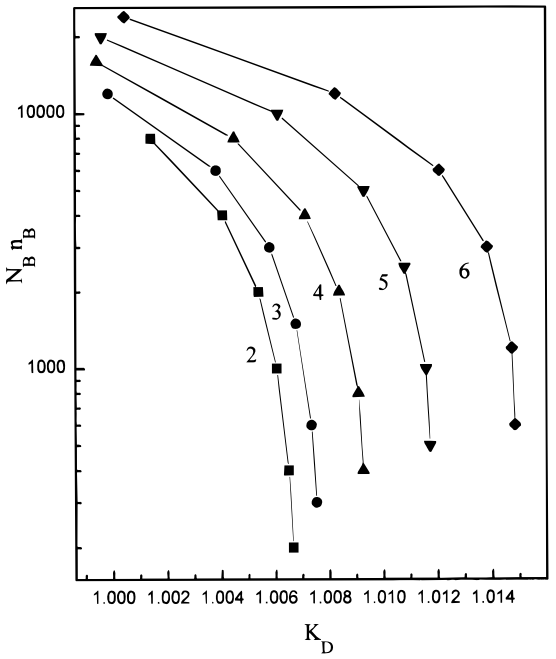

Figure 6. Partition coefficient K_D for a star homopolymer at the transition point of the infinitely long linear homopolymer, $T = 5.48$. The number of monomers in each B arm, n_B, is plotted as the ordinate and the number of arms with B monomers, N_B is varied from 2 (a homopolymer) to 6. The figure shows that moderate branching affects the compensation point only slightly. However, there should be a significant effect of branching in the exclusion limit.[6]

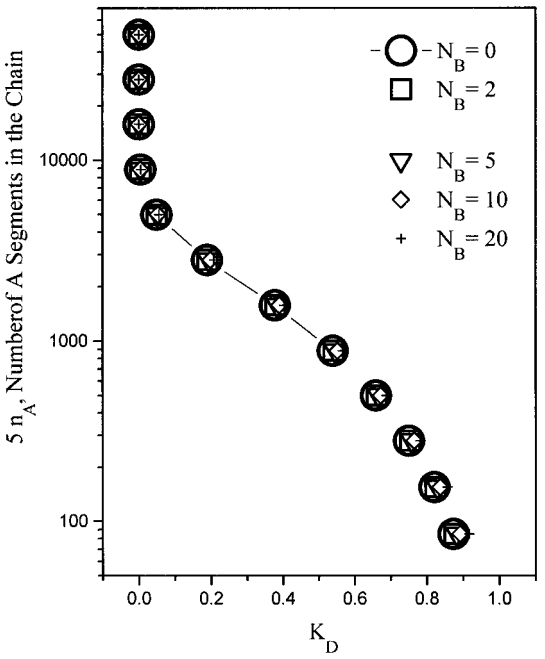

Figure 7. Partition coefficient K_D for a star copolymer where each branch is either a homopolymer of A or a homopolymer of B in a slit with a width of 50 lattice units. As in all other figures, the A monomers are excluded from the wall and the B monomers are at their compensation point, $T = 5.48$. The number of A-type arms is held at 5, and the number of arms with all B monomer, N_B, is varied from 0 to 20. For any polymer all the arms were of the same length. The ordinate is the logarithm of the total number A of segments in the chain, $n_A N_A$.

For this paper, we also consider a block copolymer star with each arm as either a homopolymer of A or a homopolymer of B. That is, the armed star is of the form $(AA...AA)_{N_A}(BB...BB)_{N_B}$ where N_A is the number of homopolymer arms made up of A segments and N_B is the number of homopolymer arms made up of B segments. Again, making the B invisible lets us only see the A, as seen in Figure 7. Figure 7 shows the K_D of a star with five A arms and between 0 and 20 arms at the compensation point. Again we show little effect of the increasing number of arms in the exclusion regime K_D and in the position of the compensation point.

H. K_D for Combs. Now we consider K_D for combs. Suppose that for every t monomers along the backbone consisting of N segments we have a side group consisting of J monomers of energy of attraction for the surface of $\Delta\epsilon_c$. The partition function for the comb-like polymer is given by

$$K_D(N) = \mathbf{U}^T(\mathbf{q}(\theta)^{t-1}\mathbf{C}(\theta))^{N/t}\mathbf{P}(0) \qquad (3.8)$$

where $\mathbf{C}(\theta)$ is defined by eq 3.9,[41] where $Q(m,J)$ is the partition function for a polymer of length J which is forced to start at level m from eq 3.10. Each of its segments has an energy of interaction with the surface of value $\Delta\epsilon_c$. For small values of J writing the functions down is best directly by means of recurrence relations.

$$\begin{aligned} Q(1,1) &= z(1-a)e^{\theta_c} + za/2, \\ Q(2,1) &= z(1-a) + zae^{\theta_c}/2 + za/2, \\ Q(3,1) &= z, \ldots \end{aligned} \qquad (3.10)$$

$$Q(1,2) = z(1-a)e^{\theta_c}Q(1,1) + Q(2,1)za/2$$

$$Q(2,2) = (zae^{\theta_c}/2)Q(1,1) + z(1-a)Q(2,1) + (za/2)Q(3,1)$$

$$Q(3,2) = (za/2)Q(2,1) + z(1-a)Q(3,1) + (za/2)Q(4,1)$$

These equations relate an n-step partition function to an $(n-1)$-step partition function by taking a first step toward, parallel to, or away from a surface. The general recurrence term is obtained if we first define θ_m as the energy that a segment sees at level m. Then

$$C(\theta) = \begin{pmatrix} (1-a)e^{\theta}Q(1,J) & {}^1/_2 ae^{\theta}Q(1,J) & & & & \\ {}^1/_2 aQ(2,J) & (1-a)Q(2,J) & {}^1/_2 aQ(2,J) & & & \\ & {}^1/_2 aQ(3,J) & (1-a)Q(3,J) & {}^1/_2 aQ(3,J) & & \\ & & \ddots & & & \\ & & & (1-a)Q(M-2,J) & {}^1/_2 aQ(M-2,J) & \\ & & & {}^1/_2 aQ(M-1,J) & (1-a)Q(M-1,J) & {}^1/_2 aQ(M-1,J) \\ & & & & {}^1/_2 ae^{\theta}Q(M,J) & (1-a)e^{\theta}Q(M,J) \end{pmatrix} \qquad (3.9)$$

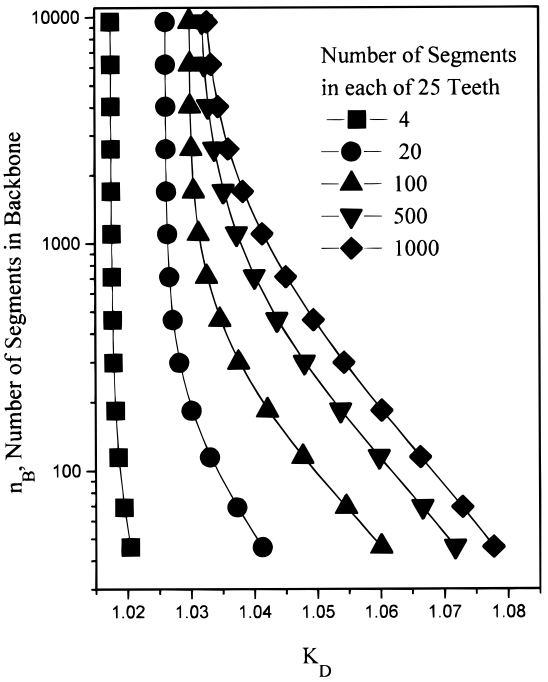

Figure 8. Partition coefficient K_D for a comb homopolymer whose teeth are at the absorption transition point of the infinitely long linear homopolymer, $T = 5.48$. The number of B-type segments in each tooth is varied from 4 to 1000. The number n_A of A-type segments in the backbone is plotted as the ordinate. The number of teeth in each chain is 25.

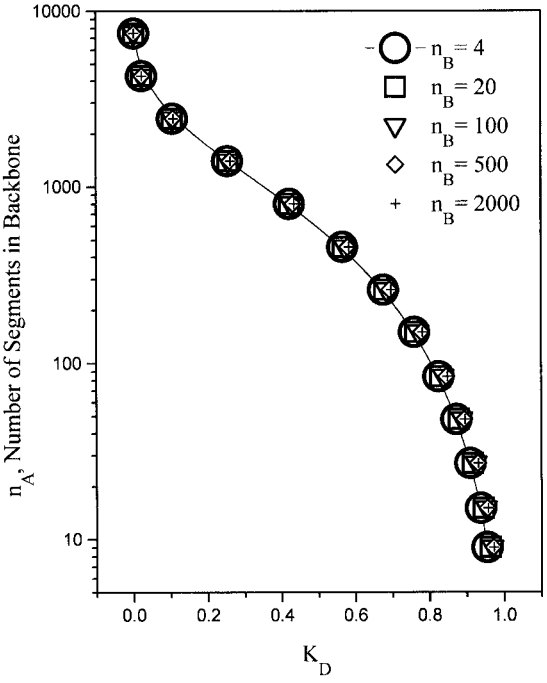

Figure 9. Partition coefficient K_D for a comb graft copolymer where the backbone is a homopolymer of A and the teeth are homopolymers of B in a slit width of 50 lattice units. As in all other figures, the A monomers are excluded from the wall and the B monomers are at the compensation point, $T = 5.48$, for their linear homopolymer of B. The number of teeth per chain is 5.

$$Q(m,J) = (za/2)\exp(\theta_{c(m-1)})Q(m-1,J-1) + z(1-a)\exp(\theta_{cm})Q(m,J-1) + (za/2)\exp(\theta_{c(m+1)})Q(m+1,J-1) \quad (3.11)$$

This equation includes all values of (m,J) if we let $Q(0,J) = Q(M+1,J) = 0$, and use eq 3.10 for $Q(m,1)$. It is obvious by an extension of the discussion at the end of section 2.1 that the backbone could be a block or random copolymer, as described above, and/or each graft could be different.

We first consider if the compensation point is changed by the architecture of the comb. In Figure 8 we show data for comb polymers with teeth grafted to the backbone. The length of the backbone and the length of the arms are varied. The partition coefficient K_D at the compensation point, $T^* = 5.48$, varies by as much as 7%. This is the largest change we have seen because of the chain architecture.

Here we only consider the case of a comb graft copolymer with a homopolymer backbone in the exclusion regime and the homopolymer teeth at the compensation point. Thus, by our naive view we should see only the backbone. Nevertheless, we see in Figure 9 that there is a small effect of the comb on the K_D on the backbone chain at the compensation point of the teeth for a comb of 5 teeth. For a comb of 25 teeth the effect is much larger, as seen in Figure 10.

We do not pursue copolymer combs or stars further in the present paper, but we plan to look at the many implications of these architectures on elution chromatography in a future paper.

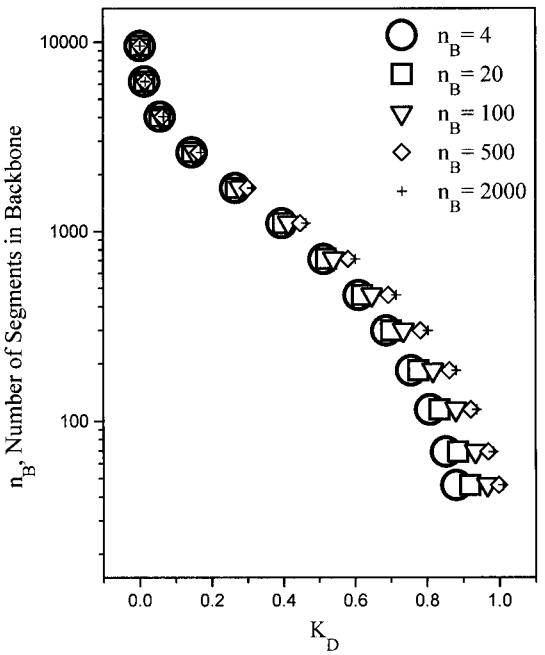

Figure 10. Partition coefficient K_D for a comb graft copolymer where the backbone is a homopolymer of A and the teeth are homopolymers of B in a slit width of 50 lattice units. As in all other figures, the A monomers are excluded from the wall and the B monomers are at their compensation point, $T = 5.48$, for the linear homopolymer of B. The number of teeth per chain is 25.

4. Discussion

In accord with experiment and previous theory we find that when SEC is extended to the vicinity of the "adsorption Θ point" (also called adsorption transition point or compensation point) regime, information on the internal structure of the polymer can be obtained. For a diblock copolymer one can choose a mixed solvent system for which one component, B, is near the adsorption compensation point and the other component, A, is in the SEC region. For this case the B portion of the molecule is invisible to the column, and only the molecular weight distribution of the A portion shows

up in the chromatograms. Thus, by choosing the solvent mixture properly, one can mask the B component.

The chromatogram for a BAB triblock copolymer again contains only the molecular weight distribution of the A component. For ABA triblocks the situation is more complicated. Here it is only approximately true that the B component is invisible to the chromatography column. The molecular weight distribution of the sum of the molecular weights of the two end blocks is obtained.

The influence of chain architecture on chain elution is also investigated. For stars the results fall easily in line with our predictions about diblock copolymers. For combs the results are more complicated. Both these architectures require further consideration.

The structure of the curves we have produced is similar to those found by Pasch and others experimentally. Does this mean the effects of the chain excluded volume and of the segment−segment interaction in the chain cancel out in K_D? If this were rigorously true, then it would suggest these effects are separable. Most likely they are absorbed into the phenomenological constants such as the critical temperature.

The elution volume curves in Figure 1 have more information than we have used. An interesting, yet unanswered, question is how this information relates to the internal structure of the polymer and the internal structure of the pores.

Finally, the present modeling and the related experiments suggest important implications about the mechanism of polymer separation chromatography. It is often considered, through arguments of universal calibration, that the mechanism of separation in SEC is not exclusively thermodynamic.[42,43] This may be the case in the strong exclusion regime, but these results and the confirming experiments suggest that this is not the case in the regime of surface adsorption. This most naive thermodynamic view of elution chromatography (we have not included polymer-polymer interactions) gives a good accounting of the main features of the phenomena. Thus, the elution volume in the regime near the surface absorption compensation point is not related to the hydrodynamic volume.

The above discussion suggests that the hydrodynamic volume may control the volume elution in the exclusion limit only. Any small amount of adsorption most likely invalidates "universal calibration" in terms of hydrodynamic volume alone. Earlier studies of the failures of universal calibration may have not considered this effect sufficiently.

Appendix A. Central Limit Theorem Approach to Understanding SEC

The probability distribution $P(t_N)$ for elution of a polymer molecule from a column of N plates at time t_N is given by the convolution operation on the distribution function p_j for the individual plates,

$$P(t_N) = \int\int\ldots\int\int \pi p_j(t_j - t_{j-1})\pi\, dt_j \; 1 \le j \le N,\; t_0 = 0 \tag{A1}$$

This formula presupposes that there is a sequential visiting of plates (no backward flow). In size exclusion chromatography p_j is given by

$$p_j(\tau) = \alpha_1 p_{j,1}(\tau) + \alpha_2 p_{j,2}(\tau) \tag{A2}$$

where for plate j, α_1 is the probability of the polymer being in the flow region and α_2 is the probability of the polymer being in a pore ($\alpha_1 + \alpha_2 = 1$). $p_{j,1}(\tau)$ is the normalized probability that the polymer molecule elutes from the flow region of plate j at time τ; $p_{j,2}(\tau)$ is the normalized probability that the polymer elutes from the pore at time τ.

Normal SEC (in the pure exclusion range) is described by $p_j(\tau)$ functions whose means and variances are finite. Then the central limit theorem ensures that $P(t_N)$ is a Gaussian distribution whose mean is given by the sum of the means of $p_j(\tau)$ and whose variance is given by the sum of the variances.

However, in the adsorption range it is known that some of the material is adsorbed in the column. This can only mean that for some of the $p_{j,2}(\tau)$ the mean values $\langle\tau\rangle$ are infinite.

$$\langle\tau\rangle = \int \tau p_{j,2}(\tau)\, d\tau = \infty \tag{A3}$$

For this case Levy flight methods must be used to determine $P(t_N)$. The work of Weiss[9] is relevant to this problem when either the first or second moments are infinite. An infinite first moment corresponds to retention of eluent in the column, while an infinite second moment corresponds to a skewing of the peak without retention.

One can generalize eq A2 to be a matrix. This is useful if one does not want to allow the polymer to jump directly from stationary phase to stationary phase, i.e. if one assumes that the polymer must reside in the mobile phase during its sojourn from stationary phase to stationary phase. Using the matrix

$$p_j(\tau) = \begin{bmatrix} \alpha_1 p_{j,11} & \alpha_2 p_{j,12} \\ \alpha_1 p_{j,21} & 0 \end{bmatrix} \tag{A4}$$

accomplishes this goal with $\alpha_1 p_{j,11} = \alpha_1 p_{j,21} = \alpha_1 p_{j,1}$, $\alpha_2 p_{j,21} = \alpha_2 p_{j,2}$. The folding theorem gives for $P(s)$, the Laplace transform of $P(t_N)$

$$P(s) = \mathbf{U}^{\mathrm{T}} \prod p_j(s) \mathbf{P} \tag{A5}$$

where $\mathbf{P}$ is the column vector 1,0 corresponding to the fact that we inject the polymer into the mobile phase and $\mathbf{U}^{\mathrm{T}}$ is the row vector 1,0 if we are detecting the polymer in the fluid phase only, and 1,1 if we are simultaneously detecting the polymer in both the fluid and stationary phases.

Appendix B. Shift of Critical Temperature T_c of Second-Order Phase Transitions Due to Finite Size and Surface Interaction

The critical temperature of many kinds of second-order phase transitions such as those described by the Ising model (phase separation in fluids, spontaneous ordering in magnets, ...) is influenced by finite size effects and surface interactions. The calculation of this shift is very similar to the calculation of K_D for polymers interacting with confining boundaries. Domb[44] first noted that the survival probability of a self-avoiding walk with confining (repulsive boundary or compensation point boundary conditions) boundaries was related to the critical point shift in the Ising model. Bray and Moore[45] and subsequently others[46−48] developed the equivalent of the Casassa model for the repulsive slit geometry for the mean-field estimate of the critical temperature shift due to finite size (this shift is equal to λ_1 in eq 2.4). The more general case of self-avoiding

walks confined to a parallel plate geometry with interacting boundaries has been treated recently by Ishinabe[49] and discussed in relation to the critical temperature shift of T_c for the Ising model. This calculations indicate that the T_c of the Ising model can be shifted either up or down depending on the magnitude of the surface interaction. Measurements on fluid condensation in confined geometries[50] and thin polymer blend layers[51] show transition temperatures which are either raised or lowered depending on the chemical nature of the surface. We also note that the glass transition temperature of thin polymer films has been observed to shift either up or down depending on surface chemistry[52] so that accurate calculations of K_D for confined polymers interacting with boundaries may provide important insights into shifts of the glass transition and the nature of the glass transition. It should be noted that no definitive theory of the glass transition exists but that the successful thermodynamic model of Gibbs−Di Marzio[53] predicts that the glass transition is second order in the Ehrenfest sense. A comparison of experimental shifts in the glass transition with those expected for second-order transitions should provide some insight into the nature of the glass transition.

As a matter of notation we note that the "adsorption Θ point" in the polymer partitioning problem is denoted as the "special transition" in the Ising model or the "normal transition" in the context of fluid mixture phase separation. Recently, there have been attempts to identify the "special transition" using surface tension measurements of polymer solutions.[47,54]

References and Notes

(1) Di Marzio, E. A.; Guttman, C. M. *Polym. Lett.* **1969**, *7*, 267; *Macromolecules* **1970**, *3*, 131.
(2) Guttman, C. M.; Di Marzio, E. A. *Macromolecules* **1970**, *3*, 681.
(3) Di Marzio, E. A.; Guttman, C. M. *J. Chromatogr.* **1971**, *55*, 83.
(4) Casassa, E. F. *J. Phys. Chem.* **1971**, *75* 3929.
(5) Casassa, E. F. *Polym. Lett.* **1967**, *5* 773.
(6) Casassa, E. F.; Tagami, Y. *Macromolecules* **1969**, *2*, 14.
(7) Di Marzio, E. A.; Rubin, R. J. *J. Chem. Phys.* **1971**, *55*, 4318.
(8) Hermans, J. J. *J. Polym. Sci. A* **1968**, *2*, 1217.
(9) Weiss, G. H. In *Transport and Relaxation in Random Materials*; Closter, J., Rubin, R. J., Shlesinger, M., Eds.; World Scientific: 1986; Singapore: pp 384−406.
(10) Entelis, S. G.; Evreinov, V. V.; Gorshkov, A. V. *Adv. Polym. Sci.* **1986**, *76*, 129.
(11) Gorshkov, A. V.; Evreinov, V. V.; Entelis, S. G. *Zh. Fiz. Khim.* **1985**, *59*, 958.
(12) Pasch, H. *Polymer* **1993**, *34*, 4095.
(13) Pasch, H.; Brinkman, C.; Gallot, Y. *Polymer* **1993**, *34*, 4100.
(14) Pasch, H.; Brinkman, C.; Much, H.; Just, U. J. *J. Chromatogr.* **1992**, *623*, 315.
(15) Zimina, T. M.; Kever, J. J.; Melenevskaya, E. Y.; Fell, A. F. *J. Chromatogr.* **1992**, *593*, 233.
(16) Gorshkov, A. V.; Much, H.; Becker, H.; Pasch, H.; Enreinov, V. V.; Entelis, S. G. *J. Chromatogr.* **1990**, *523*, 91.
(17) Skvortsov, A. M.; Gorbunov, A. A. *J. Chromatogr.* **1979**, *358*, 77−83; Skvortsov, A. M.; Gorbunov, A. A. *Polym. Sci. USSR* **1979**, *21*, 371.
(18) Skvortsov, A. M.; Zhulina, Y. B.; Gorbunov, A. A. *Polym. Sci. USSR* **1980**, *22*, 908.
(19) Gorshkov, A. V.; Much, H.; Becker, H.; Pasch, H.; Evreinov, V. V.; Entelis, S. G. *J. Chromatogr.* **1990**, *523*, 91.
(20) Douglas, J. F.; Wang, S.-Q.; Freed, K. F. *Macromolecules* **1986**, *19*, 2207.
(21) Douglas, J. F. *Macromolecules* **1989**, *22*, 3708. See Appendix B.
(22) Douglas, J. F.; Friedman, A. *Mathematics in Industrial Problems, Part 7*; The IMA Volumes in Mathematics and Its Applications, Vol. 67; Springer-Verlag: New York, 1995; p 176.
(23) Casassa, E. F. *J. Polym. Sci. B* **1967**, *5*, 773.
(24) (a) Gaylord, R. J.; Douglas, J. F. *Polym. Bull.* **1987**, *18*, 347; **1990**, *23*, 529. (b) Douglas, J. F.; McKenna, G. B. *Macromolecules* **1993**, *26*, 3282.
(25) Douglas, J. F.; Nemirovsky, A.; Freed, K. F. *Macromolecules* **1986**, *19*, 2041.
(26) (a) Rubin, R. J. *J. Res. Natl. Bur. Stds.* **1965**, *69*, 301; **1966**, *70*, 237. (b) Rubin, R. J. *J. Chem. Phys.* **1965**, *43*, 2392; **1966**, *44*, 2130.
(27) (a) Daoud, M.; deGennes, P. G. *J. Phys. (Fr.)* **1977**, *38*, 85. (b) See ref 19. (c) The average mean first-passage time of a Levy flight for which ν is variable scales as $L^{1/\nu}$. See: R. K. Getoor, *Trans. Am. Math. Soc.* **1961**, *101*, 75. Hunt, F. Y.; Douglas, J. F.; Bernal, J. *J. Math. Phys.* **1995**, *36*, 2386.
(28) See ref 20.
(29) Skvortsov, A. M.; Belen'kii, B. G.; Garkina, E. S.; Tennikov, M. B. *Vysokomol. Soyedin. A* **1978**, *20*, 678. See Figure 1.
(30) (a) Flory, P. J. *Statistical Mechanics of Chain Molecules*; Wiley-Interscience: New York, 1969. (b) Yamakawa, H. *Modern Theory of Polymer Solutions*; Harper and Row: New York, 1971. (c) Freed, K. F. *Renormalization Group Theory of Macromolecules*; Wiley: New York, 1987.
(31) Meyers, K. R.; Freed, K. F. *J. Chem. Phys.* **1993**, *98*, 2437.
(32) Rubin, R. J. *Random Walks and their Applications in the Physical and Biological Sciences. AIP Conf. Proc.* **1984**, *109* ,73. Douglas, J. F. *Macromolecules* **1989**, *22*, 3707.
(33) Birstein, T. M.; Skvortsov, A. M.; Sariban, A. M. *Macromolecules* **1976**, *9*, 892. Hoeve, C. A.; Di Marzio, E. A.; Peyser, P. J. *J. Chem. Phys.* **1965**, *42*, 2558. Zhulina, Y. E.; Gorbunov, A. A.; Skvortsov, A. M. *Polym. Sci. USSR* **1984**, *26*, 1020.
(34) Wang, Z. G. *Macromolecules* **1995**, *28*, 570.
(35) Kholodenko, A. L.; Bearden, D. N.; Douglas, J. F. *Phys. Rev. E* **1994**, *49*, 2206.
(36) Davidson, M. G.; Suter, N. W.; Dean, W. M. *Macromolecules* **1987**, *20*, 1141.
(37) Douglas, J. F. *Macromolecules* **1989**, *22*, 3707.
(38) (a) Di Marzio, E. A. *J. Chem. Phys.* **1965**, *42*, 2101. (b) Rubin, R. J. *J. Chem. Phys.* **1965**, *43*, 2392.
(39) Gorbunov, A. A.; Zhulina, E. B.; Skvortsov, A. M. *Polymer* **1977**, *23*, 1133.
(40) Di Marzio, E. A. *Macromolecules* **1993**, *26*, 4613.
(41) Di Marzio, E. A.; Guttman, C. M.; Mah, A. *Macromolecules* **1995**, *28*, 2930.
(42) Casassa, E. F. *Macromolecules* **1976**, *9*, 182.
(43) Dubin, P. L.; Principi, J. M. *Macromolecules* **1988**, *26*, 4613.
(44) Domb, C. *J. Phys. A* **1983**, *6*, 1296.
(45) Bray, A. J.; Moore, M. A. *J. Phys. A* **1978**, *11*, 715.
(46) Barber, M. N. *Phase Transitions Crit. Phenom.* **1983**, *8*, 1.
(47) Nakanishi, H.; Fisher, M. E. *J. Chem. Phys.* **1983**, *78*, 3279.
(48) Nemirovsky, A. M.; Freed, K. F. *Nucl. Phys. B* **1986**, *270*, 423; *J. Phys. A* **1989**, *19*, 591.
(49) Ishinabe, T. *J. Chem. Phys.* **1985**, *53*, 4151.
(50) (a) Meadows, M. R.; Scheibner, B. A.; Mockler, R. C.; O'Sullivan, W. J. *Phys. Rev. Lett.* **1979**, *43*, 592. (b) Reich, S.; Cohen, Y. *J. Polymer Sci., Phys. Ed.* **1981**, *19*, 1255.
(51) de Meglio, J.-M.; Taupin, C. *Macromolecules* **1989**, *22*, 2388.
(52) Orts, W. J.; van Zanten, J. H.; Wu, W. L.; Satija, S. K. *Phys. Rev. Lett.* **1993**, *71*, 867. (b) Keddie, J. L.; Jones, R. A. L.; Cory, R. A. *Europhys. Lett.* **1994**, *27*, 59.
(53) Gibbs, J. H.; Di Marzio, E. A. *J. Chem. Phys.* **1958**, *28*, 373. Di Marzio, E. A. *Ann. N.Y. Acad. Sci.* **1981**, *371*, 1. Di Marzio, E. A. Nature of the Glass Transition. In *Proceedings of the Workshop on Relaxation in Complex Systems*; Ngai, K. L., Wright, G. B., Eds.; NTIS: Springfield, VA, 1984; pp 43−52.
(54) (a) Diehl, H. W. *Phase Transitions Crit. Phenom.* **1988**, *10*, 75. (b) Fisher, M. E.; Upton, P. J. *Phys. Rev. Lett.* **1990**, *65*, 2402, 3405.

MA9602029